JGR Space Physics

TECHNICAL REPORTS: METHODS

10.1029/2020JA028409

A New Concept to Measure the Ambipolar Electric Field Driving Ionospheric Outflow

Kun Li[1], **Stein Haaland**[2,3], **and Yong Wei**[4]

[1]Planetary Environmental and Astrobiological Research Laboratory (PEARL), School of Atmospheric Sciences, Sun Yat-sen University, Zhuhai, China, [2]Max Planck Institute for Solar System Research, Göttingen, Germany, [3]Birkeland Centre for Space Science, University of Bergen, Bergen, Norway, [4]Institute of Geology and Geophysics, Chinese Academy of Sciences, Beijing, China

Key Points:

- The ambipolar electric field driving the polar wind, estimated as ~10^{-6} V m^{-1}, is difficult to measure with instruments onboard spacecraft
- We propose a new instrument concept, which extends existing technologies to measure very small parallel electric fields in space
- Our calculation suggests that the proposed concept is feasible and can be utilized to improve our understanding of the Earth's polar wind

Correspondence to:

K. Li,
likun37@mail.sysu.edu.cn

Citation:

Li, K., Haaland, S., & Wei, Y. (2021). A new concept to measure the ambipolar electric field driving ionospheric outflow. *Journal of Geophysical Research: Space Physics*, *126*, e2020JA028409. https://doi.org/10.1029/2020JA028409

Received 1 JUL 2020
Accepted 13 DEC 2020

Abstract Over the last few decades, the role of ionospheric outflow for the loss of atmospheric constituents, as a plasma supplier to the magnetosphere and hence for the evolution of the Earth's atmosphere has been recognized. A substantial amount of the outflow is thought to be caused by the presence of an ambipolar electric field aligned with the open magnetic field lines of the polar region. To better understand how the changes in outflow are influenced by the solar and geomagnetic activity, it is critical to get a better understanding of the impact of this electric field, and to be able to measure it under various conditions. However, such measurements are not possible with present techniques. In this paper, we propose a new technique to measure the tiny electric field. This technique builds on existing instrument technology but extends the capability to measure the very small electric fields. We present the underlying design concept and demonstrate that this concept is viable and able to measure the very small ambipolar electric fields thought to play a key role in the polar wind.

1. Introduction

Ionospheric outflow plays an important role in the evolution of the Earth's atmosphere andmagnetospheric dynamics (André & Cully, 2012; Brinton and Mayr, 1971; Dessler & Hanson, 1961; Engwall et al., 2009; Haaland et al., 2015; Hoffman, Dodson, Lippincott, & Hammack, 1974; Kronberg et al., 2014; Lundin et al., 2007; Welling et al., 2015; Yau & and André, 1997). Ions in the polar ionosphere can be extracted by an ambipolar electric field along the magnetic field lines (Axford, 1968; Ganguli, 1996; Yau & André, 1997, and references therein). With the magnetic field lines open and connected to the solar wind through the magnetotail, this electric field enables ions to escape from the Earth's gravity. The outflow through this mechanism is characterized by low-energy ions and is often referred to as the polar wind (Axford, 1968; Banks & Holzer, 1968). The outflow rate of the polar wind can reach up to 10^{26} s^{-1} and can be higher than the outflow in the form of conics and beams from the auroral zone. Consequently, the polar wind outflow is considered to be the main contributor to loss from the ionosphere, as well as the dominant plasma source for the magnetosphere.

The presence of an upward ambipolar electric field was first observed by the ISIS-1 spacecraft in the form of a persistent difference in upward and downward electron fluxes (Winningham & Heikkila, 1974). Subsequent observations from the Dynamic Explorer spacecraft eventually led to the interpretation that the downward moving electrons are reflected due to an upward electric field at altitudes higher than the spacecraft (Winningham & Gurgiolo, 1982). High-energy electrons can overcome the electric potential and escape from the Earth, whereas electrons with energies lower than the electric potential energy return to low altitudes. Using data obtained from the Akebono spacecraft between 300 and 3,200 km altitude, Abe et al. (1993) found a correlation between electron temperature and ion outflow velocity of the polar wind at a given altitude. This directly indicates that ions of the polar wind are accelerated by the ambipolar electric field. As the increase in ion outflow velocity is larger at a higher altitude, their results suggest a cumulative effect of the ambipolar electric field on the accelerating and eventual escape of ions from the ionosphere.

Theoretical studies based on modeling have estimated the values of the field-aligned electric potential drop due to the ambipolar electric field (Khazanov et al., 1997; Tam et al, 1995). In the models by Wilson et al. (1997) and Su et al. (1998), a field-aligned potential jump of about a few V was predicted at high altitudes (several Earth radii). A recent simulation by Khazanov et al. (2019) demonstrated that a small

and gradual potential drop of 3–4 V exists at altitudes below 3,800 km and a potential jump exists at higher altitudes. In their model, the potential jump is controlled by the ratio between hydrogen ion flux and the flux of photo electrons and polar rain electrons. The value of the simulation based potential jump is consistent with those reported by Kitamura et al. (2012), derived from the FAST spacecraft measurements. They found that the total electric potential drop above ~3,800 km altitude is frequently larger than ~10V during geomagnetically quiet periods. However, the experimental studies conducted so far have not been able to resolve the detailed structure of the potential drop and the ambipolar electric field. There is therefore a strong need for complete experimental analyses of the ambipolar electric field in addition to theoretical studies.

Direct measurements of the ambipolar electric field or total potential drop are challenging for several reasons. The main challenge is that the magnitude of the ambipolar electric field is very small. The 1–3 V total potential drop below 3,800 km altitude as reported by Su et al. (1998) would imply an average ambipolar electric field of the order of 1×10^{-6} V m^{-1}. It is not feasible to measure such small electric fields with existing techniques and present generation instrumentation.

In this paper, we present a new concept for measuring very small ambient electric fields in the polar region. The proposed instrument partly builds on existing electron drift instruments but expands their capability to also measure parallel electric fields. Such an instrument can be deployed on a spacecraft traversing the polar cap region, and in principle provide direct, in situ measurements of the ambipolar electric field. While we strongly emphasize the conceptual nature of the proposed instrument, our calculations demonstrate that the instrument principle is feasible, and can be used in future missions to study weak ambipolar electric fields in the polar wind.

This paper is organized as follows: in Section 2, we first outline the basic physics behind ionospheric outflow and the motion of an electron in an electromagnetic environment. In Section 3, we describe the working principle of the new instrument concept. Section 4 discusses a possible technical implementation and design requirements, and Section 5 summarizes this paper.

2. Forces Acting on an Electron in the Polar Cap Region

An electron in an electromagnetic environment like the terrestrial polar cap region will experience various forces. In particular relevance for ion outflow, is the acceleration along the magnetic field. This can be expressed as:

$$a_{\parallel} = \frac{dV_{\parallel}}{dt} = \frac{q}{\gamma m} E_{\parallel} - \frac{M}{\gamma m} \frac{\partial B}{\partial S} + g_{\parallel} + \vec{u}_E \cdot \frac{d\hat{b}}{dt} \tag{1}$$

The four terms on the right-hand side correspond to the parallel component of accelerations due to the ambipolar electric field, the magnetic mirror force, gravity, and the centrifugal force, respectively. In Equation 1, q is the electric charge and m is the electron mass. The term $\gamma = 1 / \sqrt{1 - V^2 / c^2}$ is the Lorentz factor with c being the speed of light in vacuum and V is the speed of the electron. $E_{\parallel}$ is the sought after ambipolar electric field. Furthermore, $g_{\parallel}$ is the parallel component of gravity. $M = \gamma m V_g^2 / 2B$ is the magnetic moment of the electron, with v_g being the gyro-rating speed of the electron. S is a unit length along the magnetic field. $\vec{u}_E = \vec{E} \times \vec{B} / B^2$ is the $\vec{E} \times \vec{B}$ convection velocity, primarily driven by solar wind-magnetosphere interaction. Finally, $\hat{b}$ is a unit vector of the magnetic field.

Not all of these forces and acceleration terms are relevant for electrons in the region of space we consider here. The acceleration due to centrifugal force is only a few m s^{-2} (see Li et al., 2012) and only becomes relevant at higher altitudes and over longer distances (Nilsson et al., 2010). Likewise, acceleration due to gravity is also smaller than 10 m s^{-2} and can be neglected.

The other two terms are of more interest for our purpose. Acceleration due to $E_{\parallel}$ (we refer to it as a_e in the following) is estimated to vary from ~10^4 to ~10^7 m s^{-2} depending on $E_{\parallel}$. Acceleration due to the magnetic mirror force, a_m, can be comparable to a_e depending on the electron gyro speed (v_g) and gradient of magnetic field strength. In the polar cap region below a few thousand km altitude, the Earth's magnetic

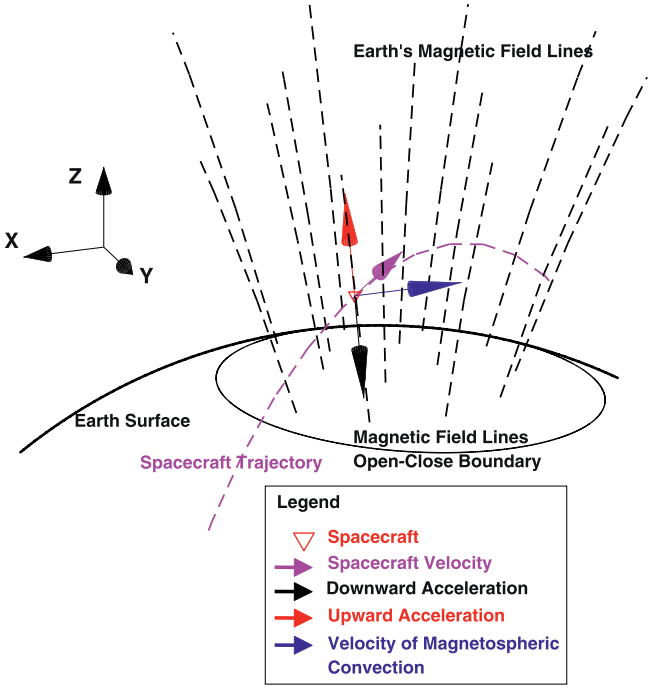

Figure 1. Schematic of a spacecraft carrying the instrument across the polar cap ionosphere. The vectors in colors show the directions of the velocities and accelerations as indicated in the legend. The upward and downward accelerations are mainly caused by the mirror force and the ambipolar electric field, respectively.

field can be approximated by a convergent (respectively divergent in the southern hemisphere) dipole field. In polar coordinates the strength of the magnetic field B as a function of the geocentric distance (r) and the polar angle from the polar axis of the northern hemisphere (θ) can be expressed as:

$$B = B_0\left(\frac{R_E}{r}\right)^3\sqrt{1+3\cos^2\theta} \tag{2}$$

where $B_0 = 3.12 \times 10^{-5}$ T is the mean value of the magnetic field at the magnetic equator of Earth's surface, $R_E = 6.731 \times 10^6$ m is the Earth's radius. Therefore, a_m calculated from the dipole field model is:

$$a_m = -\frac{M}{m}\frac{\partial B}{\partial S} = -\frac{v_g^2}{2r}\left[\frac{6\cos\theta}{\left(1+3\cos^2\theta\right)^{\frac{1}{2}}} - \frac{3\cos\theta\sin^2\theta}{\left(1+3\cos^2\theta\right)^{\frac{3}{2}}}\right] \tag{3}$$

Thus, since we ignore centrifugal acceleration and gravity, the total acceleration can be expressed as:

$$a_{\parallel} = a_e + a_m \tag{4}$$

We note that a_m depends on the electron energy and magnetic field configuration only. Provided that we operate in a near-dipole like magnetic field configuration, both these parameters can be determined with high accuracy.

3. Working Principle of the Instrument

The proposed instrument concept, hereafter referred to as the Polar Wind Electric Field Analyzer (PWEFA), partly builds on the existing Electron Drift Instrument (EDI) successfully flown on Equator-S, Cluster (Paschmann et al., 1997; Quinn et al., 2001) and the Magnetospheric MultiScale Mission (MMS – see Torbert et al., 2016). Basically, these instruments emit a set of coded electron beams with a fixed energy (in Cluster and MMS, the EDI beam energy is either 500 eV or 1 keV) perpendicular to the ambient magnetic field, and then relies on the detection of the emitted electrons after one gyro period (experience with EDI has shown that analysis can even be done for "multirunners" – electrons performing several gyrations.)

To measure the ambient magnetic field and to determine the direction of the electron beams, a precise magnetometer, similar to the Flux Gate Magnetometer (FGM) on Cluster (Balogh et al., 2001) or MMS (Russell et al., 2016) needs to be deployed along with PWEFA. On Cluster and MMS, the EDI instruments are also used to calibrate the magnetic field measurements.

Figure 1 shows a schematic plot of a spacecraft carrying the proposed instrument across the polar region of the Earth. The coordinate system used is a solar magnetospheric system (SM) in which the x-axis of the coordinate system points from the center of the Earth to the Sun, the z-axis is pointing northward and aligned with the magnetic dipole. The y-axis completes the right-handed system. To sample a range of altitudes, we envisage an elliptical orbit with apogee changing over time.

In the polar cap, which is defined by open magnetic field lines, electrons emitted from the spacecraft will experience upward and downward forces as described in Section 2. The emitted electrons will gyrate around magnetic field lines moving relative to the spacecraft. This effect on the ability to detect the return electron beam under such conditions will be discussed in Section 4.1.

As for the EDI instruments onboard Cluster and MMS, the proposed PWEFA will have an electron gun emitting coded electron beams in the direction perpendicular to the ambient magnetic field, but now with

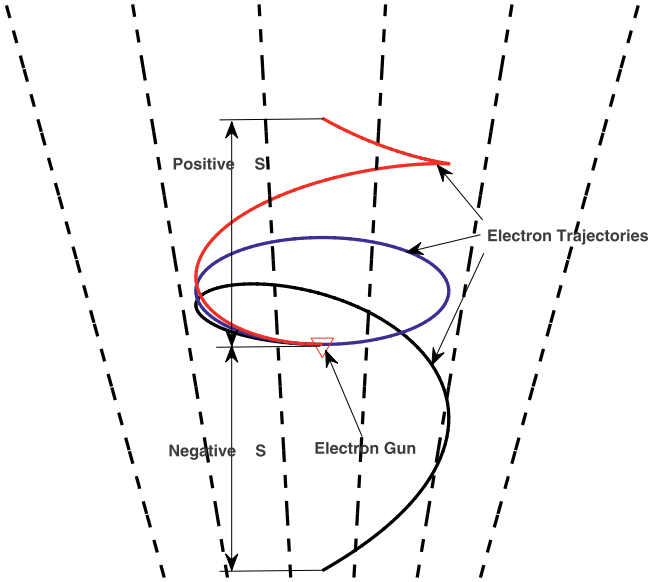

Figure 2. Definition of ΔS. Given the same ambipolar electric field and ambient magnetic field, the electron beams from the electron gun with three different energies result in three different ΔS values. By adjusting the energy of the electron beam, ΔS changes sign at a specific energy. The trajectories are for the electrons with energies at which the two forces cancel (blue), the mirror force is larger (red), and is smaller (black), than the electric force.

the possibility to sweep the beam energy, ($W = \frac{1}{2}\gamma m v_g^2$) over a wide energy range. From Equations 3 and 4, we note that different values of W will result in different values of $a_{||}$. A servo principle similar to the one used on EDI on Cluster and MMS ensures that after one gyro period, T_g, the artificially emitted electrons will return and hit the detector unit of the instrument. Due to forces across and along the magnetic field, the gyro path of emitted electrons will not be perfectly circular. In general, there will be a distance between the point of exit from the electron gun and the point where the returning electrons hit the spacecraft. The distance projected in the direction parallel to the ambient magnetic field (ΔS), and T_g can be used to derive $a_{||}$, as $a_{||} = \frac{2\Delta S}{T_g^2}$. This is illustrated in Figure 2.

ΔS can be measured by the electron detector unit, which is a combination of an electron lens and a microchannel plate surrounding the lower part of the electron gun. We will describe the design requirements for this microchannel plate detector in more detail in Section 4.4. We also note that the beam energy can be tuned (e.g., v_g^2 adjusted) so that a_m balances a_e, and the total acceleration $a_{||} = 0$. The emitted beam will then remain in the plane perpendicular to B and not move along in parallel direction at all.

Figure 3 shows plots of V_g, T_g, r_g (gyro-radius), a_m, a_e, and ΔS as a function of the electron beam energy for 500 km altitude and 90° latitude. Parameters for other locations will be discussed later. In Figures 3e–3f, the different colors show values of ΔS for $E_{||} = 10^{-7}$, 10^{-5}, and 10^{-3} V m^{-1}, respectively. In Figure 3f, we also note the transition from negative to positive values of ΔS at energies where a_m balances a_e in Equation 4. As seen in the right part of all panels, the effect of relativity will significantly affect these parameters when the electron beam energy exceeds ~10^5 eV, but as we shall see, this beam energy is not relevant for the very small electric fields in the polar wind.

In normal operation, PWEFA will emit electrons with energies sweeping from low to high (or from high to low). The energy of the emitted beam (and thus a given V_g), where ΔS flips negative to positive (or vice versa) will be used to determine $E_{||}$. For example, if the sign of ΔS changes when the energy of the electron beam is about 22.91 eV and increasing, $E_{||}$ is determined as 10^{-5} V m^{-1}.

Figure 4 shows the energy of the electron beam at which ΔS changes its sign (K_{turn}) as a function of $E_{||}$ for various altitudes and latitudes. For the latitudes from 70° to 90°, it can be seen that the changes in altitude from 300 to 900 km only result in a small variation in K_{turn}. At a given altitude, changes in latitude within 20° from the dipole axis have negligible effects on K_{turn}. Consequently, the accuracy in measuring $E_{||}$ depends almost solely on the energy span of the electron beam for each sweeping step and the spatial resolution of the electron detection unit.

4. Technical Details and Design Requirements

While the above presented technique would conceptually work (and we strongly emphasize that the design is a concept at this stage), there are challenges associated with the design of such an instrument. Below, we briefly discuss some of the design challenges and address possible solutions.

4.1. Effects of Induced Electric Fields due to Relative Motion Between Spacecraft and the Magnetic Field

One would require that T_g should be small enough so that the spacecraft does not move too far across field lines to detect the returned electron beam. This relative motion is affected by the ionospheric convection. The separation between the electron beam and the spacecraft ΔL is $\Delta L = T_g \left|\vec{u}_{sc} - \vec{u}_E\right|$, where $\vec{u}_{sc}$ is the spacecraft's velocity (a spacecraft in a nearly circular orbit at 500 km altitude travels at a speed of ~7 km

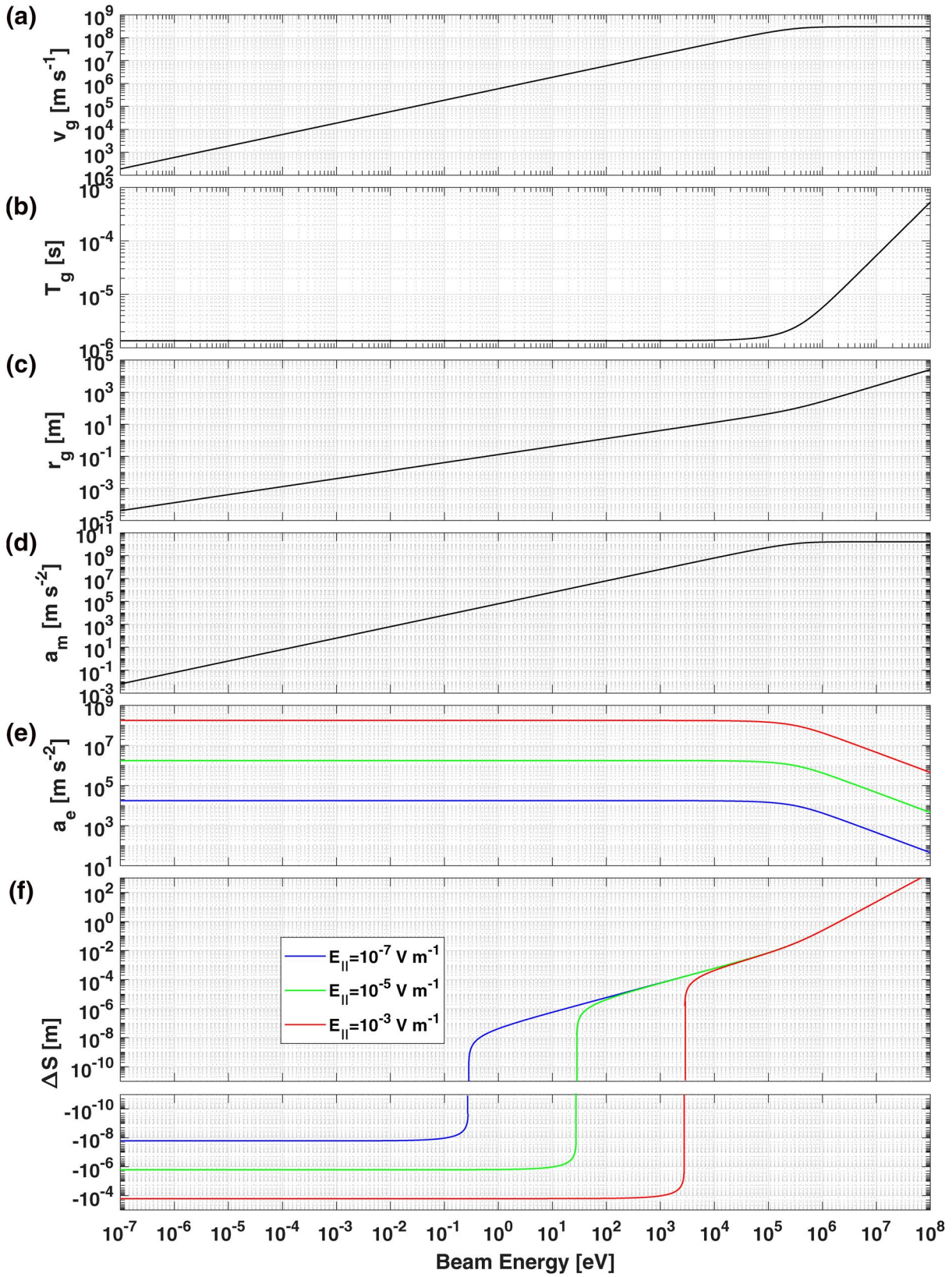

Figure 3. Parameters of electrons emitted from the electron gun as a function of initial energy for 500 km altitude and 90° latitude. Given different ambipolar electric fields ($E_{||}$), a_e varies (shown in Figure 3e) and subsequently ΔS changes sign at a given energy (shown in Figure 3f). The energy at which ΔS change its sign can be used to determine $E_{||}$.

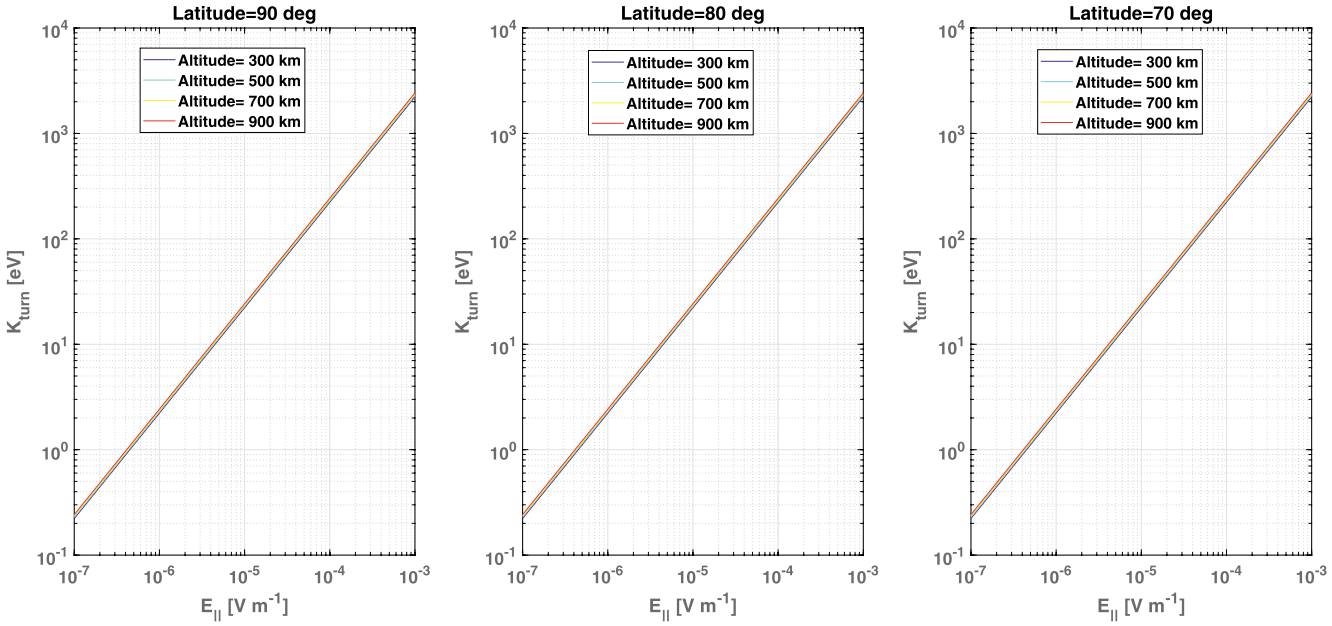

Figure 4. The energy of the electron beam at which ΔS changes its sign (K_{turn}) as functions of $E_{||}$ for different altitudes and latitudes. The values of K_{turn} are calculated from Equations 3 and 4.

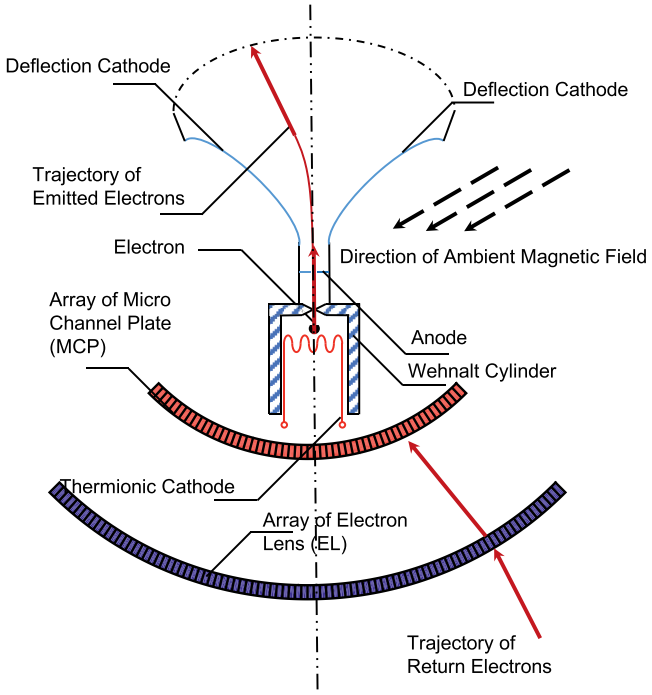

Figure 5. A cross-section view of the cylindrical symmetric instrument, including the electron gun, the array of electron lenses, and the array of microchannel plates. Electrons emitted from the electron gun can be steered by the deflection cathodes into a direction perpendicular to the ambient magnetic field. The electrons return after one gyro period and hit the electron lens, which magnifies the small displacements caused by the imbalanced accelerations along the ambient magnetic field. The magnified displacements are big enough to be resolved by the microchannel plates.

s^{-1}), $\vec{u}_E$ is the ionospheric convection (rarely more than 1 km s^{-1} in these altitudes). These figures lead to a maximum value of ΔL about 10^{-2}m when the energy of the electron beam is lower than 10^5 eV. Therefore, the return electron beam can be detected by an MCP if the size of the MCP is larger than 10^{-2} m in the direction of $\vec{u}_{sc} - \vec{u}_E$.

4.2. Size of the Electron gun and the Electron Detection Unit

The size of the electron gun and the electron detection unit are important parameters for the instrument. The instrument needs to be smaller than the gyro-radius of the electron beam, r_g, so that the electrons can leave from the electron gun on one side, and hit the electron detector unit on the other side after one gyro-period (see Figure 5). Given a fixed size of the instrument, the lower limit of r_g constrains the minimum $E_{||}$ the instrument can measure. As demonstrated in Figure 4, measuring $E_{||}$ as small as 10^{-6} V m^{-1} requires an electron beam with energy of about 3 eV, which corresponds to a gyro-radius of about 10 cm (Figure 3c). Consequently, the whole instrument unit has to be smaller than 20 cm in diameter. A less stringent $E_{||}$ resolution, e.g., 10^{-5} V m^{-1} would work with a higher beam energy, and allow a larger instrument size.

4.3. Beam Steering Mechanism

An important property of the electron gun is the ability to rapidly orient the electron beam in the direction perpendicular to the ambient magnetic field. This can be achieved by applying deflection electrodes beside the path of electrons (see details in Figure 5). The same technology has been successfully used on the EDI for Equator-S, Cluster, and MMS spacecraft (see Paschmann et al., 1997; Quinn et al., 2001; Torbert et al., 2016). Electrons are emitted from a thermionic cathode contained in a Wehnalt cylinder, which is a circular cylinder with an aperture at the center of one of

its bases. The Wehnalt cylinder has a negative electric potential and repels electrons. Only electrons from the thermionic cathode that are aligned with the long axis as well as the aperture of the cylinder will pass through. As a result, an electron beam in the direction parallel to the long axis of the Wehnalt cylinder is generated. An anode with positive voltages is used to accelerate the electron beam to the desired energies.

Unlike the EDI instruments onboard Cluster and MMS, the proposed instrument does not need a fully 180° steerable electron beam. Recall that Cluster and MMS probe large regions of the magnetosphere, and the magnetic field can have any direction relative to axis of the electron gun. As noted above, EDI beam energies on Cluster and MMS are 500 or 1,000 eV, and typical gyro radii of the order of several km. Beam spread then becomes an issue (see e.g., Kletzing et al., 1994), and the returned beam is actually an elongated sheet along the magnetic field although beam is refocused after one gyroration in the plane perpendicular to the magnetic field.

In the target region of our new proposed instrument concept (the polar cap), the magnetic field is stable and almost radial. The spacecraft on which the instrument is to be deployed, traverse these field lines almost perpendicular. A much smaller range of beam directions (and detector unit) is, therefore, acceptable. Better focusing of the beam should then be possible. Combined with the much smaller beam energies, and thus smaller gyro radius of the emitted electrons, the elongation in parallel direction of return beam becomes smaller.

For PWEFA, the design requirement is that the beam is narrow enough, and has a spread characteristic that ensures that the displacement, ΔS, can be resolved by the detector unit (described in the next section). While we think that the beam spread design requirement can be met by using the combination of a thermionic cathode technique, and a detector system able to detect the center of the "spread" beam, a solid state emitter technique may be an alternative. In particular, the double-gate field emitter cathode as described and tested by Lee et al. (2018) and Tsujino et al. (2016) is a promising technique. The actual emitter tip of the double-gate field emitter cathode has a curvature radius of only a few nanometers, and generates highly collimated electron beams with angular spread much smaller than that of the EDI instruments on Cluster and MMS. The spread in energy of the beam is just a fraction of an electron volt. While not tested in space environments, deployment of this technique should be feasible.

Stability and uniformity of deflection plate voltages are crucial to be able to accurately steer and focus electron beams with energies of only a few eV. As the voltages are controlled by the instrument's electronics, electronics with fast response and high precision, combined with materials with high, uniform conductivity and low capacitance are needed. Influence from photoelectrons should be reduced by minimizing sunlit surface areas.

4.4. Unit of Electron Lens Combined with Microchannel Plate (EL-MCP)

Our calculations show that measuring $E_{||}$ of the order of 10^{-6} V m^{-1} require a Micro Channel Plate (MCP) detector unit capable of resolving ΔS values of the order of 10^{-8} m. With current MCP based technology, this is not yet possible. The best spatial resolution of an MCP-based detector achieved in space environment so far is approximately 1×10^{-5} m (Popecki et al., 2016; Tremsin & Vallerga, 2019). This limits our ability to make an instrument capable of measuring values of $E_{||}$ smaller than about 10^{-3} V m^{-1}. One possible solution to circumvent this constraint is therefore to use electron optics to magnify ΔS prior to detection by the MCP measurements.

Here we propose to use an array of electron lenses. The perspective view of this spherical symmetric arrays of electron lenses (EL) and MCPs is shown in Figure 6. The MCPs are installed on a sphere with a smaller radius which shares the same origin as the sphere for the electron lenses. Figure 7 shows the details of one of the electron lenses. Similar to the electrostatic Einzel lens (Heddle, 2000), each electron lens consists of two apertures aligned to the radial direction (shown as $\hat{r}$). Two pairs of plates with different electric potential (V1 and V2) are aligned perpendicular to the polar direction ($\hat{\theta}$). The two pairs of plates are separated in the radial direction, and each pair of plates are separated in the direction of the polar angle. There is no obstacle in the azimuthal direction for electrons. To fit all of the electron lenses in a sphere, the aperture for electrons traveling in is slightly larger than that for electrons traveling out.

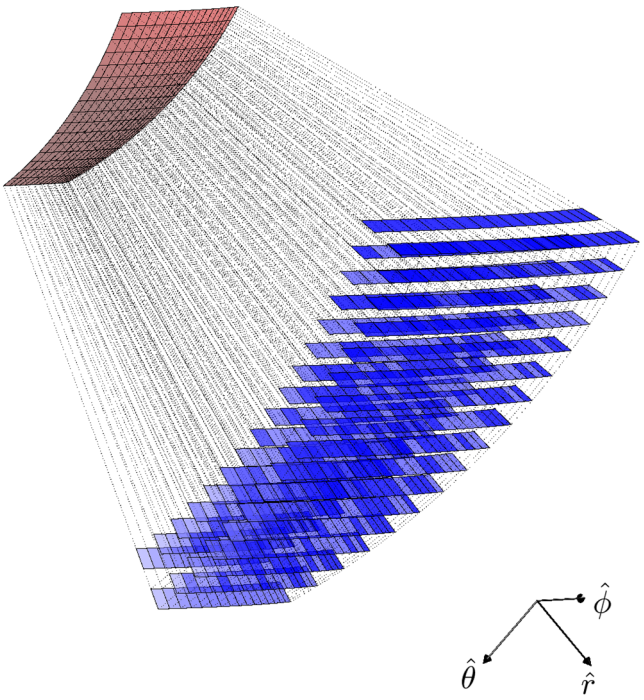

Figure 6. A perspective view of parts of the spherical electron detection unit, which includes the array of micro channel plates (MCP, in red) and the array of electron lenses (EL, in blue). The three vectors at the bottom right indicate the radial ($\hat{r}$), polar ($\hat{\theta}$) and azimuthal ($\hat{\phi}$) directions for (θ, ϕ)=(155, 45) degrees. Only the parts with the polar angle between 135° and 175° and the azimuthal angle between 30° and 60° are shown in this figure, although the entire electron detection unit covers the sphere with $\theta > 135°$ (see Figure 5). The upper part of the electron gun occupies the sphere with $\theta < 45°$. Each EL is composed of two pairs of plates with different electric potentials; its purpose is to magnify beam displacements ΔS smaller than approximately 10^{-5} m, prior to direct measurements by the MCP.

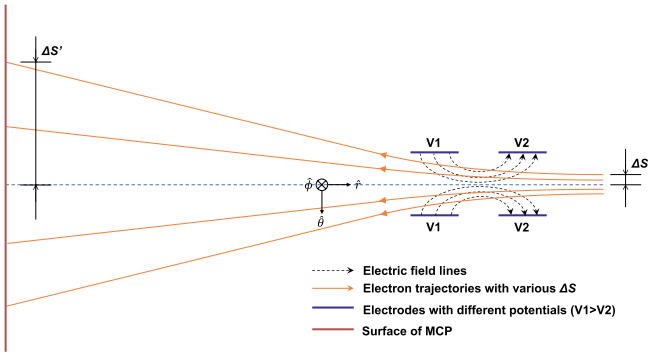

Figure 7. A cross-sectional view of each electron lens (EL). The EL consists of two pairs of plates with different electric potentials (V1>V2 and V1>0). Electrons entering the EL with a small ΔS (as indicated on the right-hand side) will be diverted by the electric fields and hit the surface of the MCP with a large $\Delta S'$. The magnification, defined as $\Delta S'/\Delta S$, needs to be approximately 10^4.

Figure 7 illustrates a situation for V1>V2 and V1>0. Electrons entering the EL from the right, and a small ΔS relative to the central dashed line, are accelerated in the polar direction. As electrons exit the EL to the left of the plates with potential of V1, they are diverted and hit the MCP with a spread $\Delta S'$. The magnification (calculated by $\Delta S'/\Delta S$) has to be about 10^4. This can be achieved by adjusting V1, V2, the distances between the two pairs of plates, and the distances between the EL and the MCP. A similar technology with a magnification up to 10^3 for cold atoms has already been published by Stecker et al. (2017). We infer that magnification of the displacement of electrons can be even larger because electrons have a much smaller mass than atoms.

4.5. Some Notes About Operation in a Nonideal Plasma Environment

To emphasize the concept and possible design solutions, we have for simplicity assumed a near-ideal operating environment, with a strong and stable dipole-like magnetic field which allows for an accurate determination of the mirror force term in Equation 1. We have also assumed a situation with no significant background electron content.

From our experience with the EDI instrument onboard Cluster, we know that the latter assumptions are not completely unreasonable at high altitudes above the polar cap regions. In lower altitudes of the polar cap region, there will be a higher background electron flux and more attenuation of the artificially emitted electron beam, possibly causing loss of the beam signal. For the small gyro radii used here, this is less of an issue compared to the EDI instruments on Cluster and MMS, since the beam has a very short travel distance. Increasing the beam current and decreasing the angular spread of the beam can also partly compensate for some of the attenuation.

A second concern is that photoelectrons and secondary electrons with energies close to the beam energy can be generated at or near the electron detector unit, and possibly making it difficult to detect and decode the beam signals. Alternating beam coding may help increasing the signal-to-noise ratio (SNR). The instruments flown on Cluster and MMS utilized a rather simple, correlation technique to increase the SNR; Beam detection is based on a positive correlation between the emitted and received electron beam code. Recent technical advances in signal processing, making use of more powerful onboard digital processing units may be used in a future mission to improve the SNR for detection of the returning electron beam.

4.6. Issues with the Smallest Detectable $E_{||}$

As shown in the above calculation, a target of 10^{-6} V m^{-1} for $E_{||}$ implies an energy of about 3 eV for the emitted electron beam. Such small energies can be affected by small scale, local electric potential structures around the instrument. According to Anderson et al. (1994), the electric potential of the Dynamics Explorer 2 spacecraft operating at altitudes between 300 km and 1,000 km was negative and rarely exceeded 1 V negative if there is no significant particle precipitation. However, potentials on the instrument can be different if the instrument is differently shaped.

In a typical plasma environment of the ionosphere, electric currents on the surface of the an instrument are dominated by bombardment of

background plasma. Ions with small thermal speeds are considered stationary to spacecraft, and only ram surfaces of the instrument will be hit by ions. In contrast, all surfaces of the instrument will be hit by electrons, since their thermal speeds are much larger than that of the spacecraft. The voltage on the instrument $\varnothing$ due to collecting charged particles from background plasma can be calculated as:

$$\varnothing = -\frac{kT_e}{e}\ln\left[\frac{A_e}{A_i}\left(\frac{kT_e}{2\pi m_e v_{sc}^2}\right)^{\frac{1}{2}}\right] \tag{5}$$

where A_e and A_i are the areas on the instrument collecting electrons and ions, respectively. k is the Boltzmann constant. m_e and T_e are mass and temperature of electrons, respectively. v_{sc} is the speed of the spacecraft. Considering a spherical surface of a spacecraft and $T_e = 1{,}500$ K, the calculated $\varnothing$ is -0.458 V (Anderson, 2012). Thus, to minimize any unwanted potentials caused by ambient electrons and ions hitting the instrument and spacecraft, the surface area of the instrument and spacecraft should be kept small. Highly conducting surface areas combined with active potential controls like the Plasma Source Instrument (PSI) flown on Polar (Su et al., 1998) or Active Spacecraft Control (ASPOC) flown on Cluster (Riedler et al., 1997) may also help reducing effects of externally generated, unwanted potentials and spacecraft charging effects.

Spacecraft induced electric and magnetic fields also affect motion of electrons close to the spacecraft. These effects can be reduced by putting the instrument on a sufficiently long boom, as often done with magnetometers to reduce the effect of spacecraft induced magnetic fields.

A relaxed $E_{||}$ target, e.g., of the order of 10^{-5} V m^{-1} or larger, will allow higher beam energies, and measurements will be less affected by electric potential structures near the instrument or nonuniform deflection plate voltages in the electron gun. Realization of the proposed instrument obviously implies a balance between science objectives (ability to measure very small electric fields) and technical feasibility.

5. Summary

The loss of atmospheric ions from the Earth's polar region is mainly attributed to the ambipolar electric field along the magnetic field. This electric field is generated by the charge separation between electrons and ions, and can be as low as 10^{-6} V m^{-1}. Presently, electric field measurements onboard spacecraft typically rely on measurements of electric potential between the two separated probes in plasma. To obtain accurate measurements of very small electric fields, the distance between the two probes will have to be very large. This introduces difficulties in the structural design of spacecraft due to imbalance heating and irradiation on different parts of the spacecraft, and is presently not feasible. An alternative indirect method in which the electric field is derived from plasma instruments and particle spectra is also not accurate enough.

To address this dilemma, we propose a new technique to measure the small ambipolar electric field in the polar cap region. The proposed instrument – polar wind electric field analyzer (PWEFA), builds on the experience from the electron drift instruments (EDI) flown onboard the Equator-S, Cluster, and MMS spacecraft, but adds the capability to measure very small parallel electric fields. The proposed instrument emits electron beams in the direction perpendicular to the magnetic field and measures the movements of the returning electron beam to determine the ambipolar electric field. This instrument combines existing technologies, including an electron gun, an array of electron lenses, and an array of micro channel plates with a spatial resolution as high as possible.

While we once again emphasize that the instrument presented here is conceptual, our calculations demonstrate that the proposed design concept is feasible. It should be possible to construct such an instrument using present technology. The ability to measure very small parallel electric fields will significantly advance our knowledge about acceleration mechanisms responsible for low energy ionospheric outflow.

Finally, although our scientific interests, and thus the motivation for this study, are focused around ionospheric outflow and the very small ambient electric field driving the polar wind, deployment in other regions of space are also conceivable. The measurement principle – determining the balance between upward forces from the mirror force and downward force by the electric field acting on an electron – should work in

any region with similar magnetic topology. For example, the nearby cusp and auroral regions have similar magnetic topologies with nearly radial magnetic fields and parallel electric fields that can be orders of magnitude larger. Although the underlying mechanisms generating field aligned potentials in these regions may be different from those of the polar wind, the proposed instrument concept should be able to measure also in this regions. As alluded to in the calculations above, a lower measurement resolution also relaxes some of the instrument design parameters.

Data Availability Statement

The data used in this work are obtained from the theoretic calculations described in the text.

Acknowledgments
This work was supported by the Strategic Priority Research Program of Chinese Academy of Sciences (Grant XDA17010201), the preresearch project on Civil Aerospace Technologies No. D020104 funded by China's National Space Administration, and the National Natural Scientific Foundation of China under Grant 41704164. Research efforts by S. Haaland were supported by the Norwegian Research Council under Grant 223252 and the Deutsches Zentrum für Luft- und Raumfahrt (DLR) under Grant 50 OC 1602. Research efforts by W. Y. were supported by the National Natural Scientific Foundation of China under Grant 41525016.

References

Abe, T., Whalen, B. A., Yau, A. W., Watanabe, S., Sagawa, E., & Oyama, K. I. (1993). Altitude profile of the polar wind velocity and its relationship to ionospheric conditions. *Geophysical Research Letters*, *20*, 34. https://doi.org/10.1029/93GL02837

Anderson, P. C. (2012). Characteristics of spacecraft charging in low Earth orbit. *Journal of Geophysical Research*, *117*, A07308. https://doi.org/10.1029/2011JA016875

Anderson, P. C., Hanson, W. B., & Hoegy, W. R. (1994). Spacecraft potential effects on the Dynamic Explorer 2 satellite. *Journal of Geophysical Research*, *99*, 3985. https://doi.org/10.1029/93JA02104

André, M., & Cully, C. M. (2012). Low-energy ions: A previously hidden solar system particle population. *Geophysical Research Letters*, *39*, L03101. https://doi/:10.1029/2011GL050242

Axford, W. I. (1968). The polar wind and the terrestrial helium budget. *Journal of Geophysical Research*, *73*, 6855–6859. https://doi.org/10.1029/JA073i021p06855

Balogh, A., Carr, C. M., Acuña, M. H., Dunlop, M. W., Beek, T. J., Brown, P., et al. (2001). The Cluster magnetic field investigation: overview of in-flight performance and initial results. *Annales Geophysicae*, *19*, 1207–1217. https://doi.org/10.5194/angeo-19-1207-2001

Banks, P. M., & Holzer, T. E. (1968). The polar wind. *Journal of Geophysical Research*, *73*, 21. https://doi.org/10.1029/JA073i021p06846

Brinton, H. C. J. M. G., & Mayr, H. G. (1971). Altitude variation of ion composition in the mid-latitude trough region: Evidence for upward plasma flow. *Journal of Geophysical Research*, *76*, 3738. https://doi.org/10.1029/JA076i016p03738

Dessler, A. J., & Hanson, W. B. (1961). Possible energy source for the aurora. *Astrophysical Journal*, *134*, 1024–1025. https://doi.org/10.1086/147241

Engwall, E., Eriksson, A. I., Cully, C. M., André, M., Puhl-Quinn, P. A., Torbert, R., & Vaith, H. (2009). Earth's ionospheric outflow dominated by hidden cold plasma. *Nature Geoscience*, *2*(1), 24–27. https://doi.org/10.1038/NGEO387

Ganguli, S. B. (1996). The polar wind. *Reviews of Geophysics*, *34*, 311–348. https://doi.org/10.1029/96RG00497

Haaland, S., Eriksson, A., André, M., Maes, L., Baddeley, L., Barakat, A., et al. (2015). Estimation of cold plasma outflow during geomagnetic storms. *Journal of Geophysical Research: Space Physics*, *120*(12), 10622–10639. https://doi.org/10.1002/2015ja021810

Heddle, D. W. O. (2000). *Electrostatic lens systems* (2nd ed.). Boca Raton: CRC Press, Taylor & Francis Group, LLC. ISBN: 0750306971. https://doi.org/10.1201/NOE0750306973

Hoffman, J. H., Dodson, W. H., Lippincott, C. R., & Hammack, H. D. (1974). Initial ion composition results from Isis 2 satellite. *Journal of Geophysical Research*, *79*(28), 4246–4251. https://doi.org/10.1029/JA079i028p04246

Khazanov, G. V., Krivorutsky, E. N., & Sibeck, D. G. (2019). Formation of the potential jump over the geomagnetically quiet sunlit polar cap region. *Journal of Geophysical Research: Space Physics*, *124*, 4384–4401. https://doi.org/10.1029/2019JA026576

Khazanov, G. V., Liemohn, M. W., & Moore, T. E. (1997). Photoelectron effects on the self-consistent potential in the collisionless polar wind. *Journal of Geophysical Research*, *102*(A4), 7509–7521. https://doi.org/10.1029/96JA03343

Kitamura, N., Seki, K., Nishimura, Y., Terada, N., Ono, T., Hori, T., & Strangeway, R. J. (2012). Photoelectron flows in the polar wind during geomagnetically quiet periods. *Journal of Geophysical Research*, *117*, A07214. https://doi.org/10.1029/2011JA017459

Kletzing, C. A., Paschmann, G., Boehm, M. H., Haerendel, G., Sckopke, N., Baumjohann, W., et al. (1994). Electric fields derived from electron drift measurements. *Geophysical Research Letters*, *21*(17), 1863–1866. https://doi.org/10.1029/94GL01072

Kronberg, E. A., Ashour-Abdalla, M., Dandouras, I., Delcourt, D. C., Grigorenko, E. E., Kistler, L. M., et al. (2014). Circulation of heavy ions and their dynamical effects in the magnetosphere: Recent observations and models. *Space Science Reviews*, *184*(1–4), 173–235. https://doi.org/10.1007/s11241-014-0104-0

Lee, C., Tsujino, S., & Dwayne Miller, R. J. (2018). Transmission low-energy electron diffraction using double-gated single nanotip field emitter. *Applied Physics Letters*, *113*, 013505. https://doi.org/10.1063/1.5030889

Li, K., Haaland, S., Eriksson, A., André, M., Engwall, E., Wei, Y., et al. (2012). On the ionospheric source region of cold ion outflow. *Geophysical Research Letters*, *39*, L18102. https://doi.org/10.1029/2012GL053297

Lundin, R., Lammer, H., & Ribas, I. (2007). Planetary magnetic fields and solar forcing: Implications for Atmospheric Evolution. *Space Science Reviews*, *129*, 245–278. https://doi.org/10.1007/s11214-007-9176-4

Nilsson, H., Engwall, E., Eriksson, A., Puhl-Quinn, P. A., & Arvelius, S. (2010). Centrifugal acceleration in the magnetotail lobes. *Annales Geophysicae*, *28*, 569–576. https://doi.org/10.5194/angeo-28-569-2010

Paschmann, G., Melzner, F., Frenzel, R., Vaith, H., Parigger, P., Pagel, U., et al. (1997). The electron drift instrument for Cluster. *Space Science Reviews*, *79*, 233–269. https://doi.org/10.1023/A:1004917512774

Popecki, M. A., Adams, B., Craven, C. A., Cremer, T., Foley, M. R., Lyashenko, A., et al. (2016). Microchannel plate fabrication using glass capillary arrays with atomic layer deposition films for resistance and gain. *Journal of Geophysical Research: Space Physics*, *212*, 7449–7460. https://doi.org/10.1002/2016JA022580

Quinn, J. M., Paschmann, G., Torbert, R. B., Vaith, H., McIlwain, C. E., Haerendel, G., et al. (2001). Cluster EDI convection measurements across the high-latitude plasma sheet boundary at midnight. *Annales Geophysicae*, *19*, 1669–1681. https://doi.org/10.5194/angeo-19-1669-2001

Riedler, W., Torkar, K., Ruedenauer, F., Fehringer, M., Pedersen, A., Schmidt, R, et al. (1997). Active spacecraft potential control. *Space Science Reviews*, *79*, 271–302.

Russell, C. T., Anderson, B. J., Baumjohann, W., Bromund, K. R., Dearborn, D., Fischer, D., et al. (2016). The magnetospheric multiscale magnetometers. *Space Science Reviews*, *199*, 189–256. https://doi.org/10.1007/s11214-014-0057-3

Stecker, M., Schefzyk, H., Fortágh, J., & Günther, A. (2017). A high resolution ion microscope for cold atoms. *New Journal of Physics*, *19*, 043020. https://doi.org/10.1088/1367-2630/aa674

Su, Y.-J., Horwitz, J. L., Wilson, G. R., Richards, P. G., Brown, D. G., & Ho, C. W. (1998). Self-consistent simulation of the photoelectron-driven polar wind from 120 km to 9 RE altitude. *Journal of Geophysical Research*, *103*, 2279–2296. https://doi.org/10.1029/97JA03085

Tam, S. W. Y., Yasseen, F., Chang, T., & Ganguli, S. B. (1995). Self-consistent kinetic photoelectron effects on the polar wind. *Geophysical Research Letters*, *22*(16), 2107–2110. https://doi.org/10.1029/95GL01846

Torbert, R. B., Vaith, H., Granoff, M., Widholm, M., Gaidos, J. A., Briggs, B. H., et al. (2016). The electron drift instrument for MMS. *Space Science Reviews*, *199*, 283–305. https://doi.org/10.1007/s11241-015-0182-7

Tremsin, A. S., & Vallerga, J. V. (2019). Unique capabilities and applications of microchannel plate (MCP) detectors with Medipix/Timepix readout. *Radiation Measurements*, *130*. https://doi.org/10.1016/j.radmeas.2019.106228

Tsujino, S., Das Kanungo, P., Monshipouri, M., Lee, C., & Dwayne Miller, R. J. (2016). Measurement of transverse emittance and coherence of double-gate field emitter array cathodes. *Nature Communications*, *7*, 13976. https://doi.org/10.1038/ncomms13976

Wilson, G. R., Khazanov, G., & Horwitz, J. L. (1997). Achieving zero current on open flux tubes carrying large photoelectron fluxes. *Geophysical Research Letters*, *24*, 1183.

Winningham, J. D., & Gurgiolo, C. (1982). DE-2 photoelectron measurements consistent with a large scale parallel electric field over the polar cap. *Geophysical Research Letters*, *9*(9), 977–979. https://doi.org/10.1029/GL009i009p00977

Winningham, J. D., & Heikkila, W. J. (1974). Polar cap auroral electron fluxes observed with Isis 1. *Journal of Geophysical Research*, *79*, 7. https://doi.org/10.1029/JA079i007p00949

Yau, A. W., & André, M. (1997). Sources of ion outflow in the high latitude ionosphere. *Space Science Reviews*, *80*, 1–25. https://doi.org/10.1023/A:100947203046